Investigation of carbon and silicon partitioning on ferrite hardening in a medium silicon low alloy ferrite-martensite dual-phase steel

A. Khajesarvi [1] , S. S. Ghasemi Banadkouki *[2]

Department of Mining and Metallurgical Engineering, Yazd University, University Blvd, Safayieh, Yazd, PO Box: 98195 – 741, Iran

Abstract

In this paper, the micromechanical behavior of ferrite microphase was evaluated in conjunction with carbon, and silicon partitioning occurred during prior austenite to ferrite phase transformation using microhardness measurements supplemented by light observation and field-emission scanning electron microscopy equipped with X-ray energy dispersive spectroscopy (EDS). For this purpose, at first, the samples were austenitized at 900°C for 15 min and then air-cooled (normalized) to room temperature in order to develop more starting homogeneous microstructural features in the proposed heat-treated samples. The wide variety of ferrite-martensite dual-phase (DP) samples containing different volume fractions of ferrite and martensite microphases developed using step-quenching heat treatment processes at 750, 720, 700, and 680°C for 5 min isothermal holding time with the subsequent water quenching after being austenitized at 900°C for 15 min in the same conditions as to the direct water-quenched (WQ) samples. The experimental results showed that, the average ferrite microhardness from the central location of ferrite grains toward the ferrite area near the prior α/γ interfaces has been increased from 122 to 145HV_{1g} for DP samples treated at 720°C for 5 min holding time. The carbon and silicon concentrations from central regions of ferrite grains toward the α/γ interface are decreased from 5.97 to 4.14 EDSNs and 0.89 to 0.45 EDSNs, respectively, while the associated ferrite hardening response was abnormally higher in comparison to that of the central regions of ferrite grains. This abnormal higher trend in ferrite hardness with lower carbon and silicon concentrations was attributed to the higher ferrite/martensite interaction of the ferrite area adjacent to the martensite generated during martensitic phase transformation.

Keywords:Ferrite-martensite; dual-phase microstructure; microhardness; hardening variation; alloying element partitioning.

1. Introduction

Low alloy dual-phase (DP) steels with ferrite–martensite microstructures have been developed over the past few decades ago and offered an impressive combinations of mechanical properties such as continuous yielding behavior and superior strength–ductility combinations[1-7]. Low carbon ferrite-martensite DP steels are one of the family members of low alloy work-hardenable steels with a good combination of strength and ductility, which is a suitable material for sheet forming operations, particularly in the automotive industry[8-12]. The ferrite and martensite microphases are arranged in a manner that the soft ferrite matrix phase

**Corresponding author*
Email:sghasemi@yazd.ac.ir
Address: Department of Mining and Metallurgical Engineering, Yazd University, University Blvd, Safayieh, Yazd, PO Box: 98195 – 741, Iran
1. Ph.D. Candidate
2. Associate professor

plays the role of ductility, and the hardening phase is martensite, of course in some cases, the microstructures may contain small amounts of bainite or retained austenite as well[4,13-14].

One of the heat treatment methods for developing ferrite-martensite DP microstructures is step-quenching heat treatment cycles[15-16]. In the step-quench path, at first, the steel samples are heated to the single-phase of austenite region for a particular temperature and time followed by step-quenching in a molten salt bath at the various isothermal temperature corresponding to the $\alpha + \gamma$ DP region and kept for a predetermined period of holding time followed with subsequent quenching in water or hot oil to room temperature. In this heat-treated process, by cooling the samples from the single-phase of austenite region to the DP of $\alpha + \gamma$ region, the ferrite phase partially nucleates and grows from the prior austenite grain boundaries developing ferrite and austenite DP microstructures containing various volume fraction of ferrite. After quenching samples from step quenching temperature in water or hot oil, the DP microstructures containing hard martensite phase surrounded by soft ferrite matrix are formed in the heat-treated samples[17-19].

In general, the strength of ferrite-martensite DP steels is governed not only by the strength and volume fraction of ferrite and martensite microconstituents but also by the interaction of these microphases with each other which in turn can be controlled by a thermal coefficient mismatch of microphases, the nature and atomic bonding between microphases, and the heat treating cycles[20]. The interaction between ferrite and martensite microconstituents has been believed to introduce a significant density of unpinned dislocations generated within ferrite during subsequent martensite phase transformation [21-22]. These dislocated ferrite areas are influenced by some of the other variable microstructural parameters such as ferrite morphology and ferrite volume fraction, causing a significant variation of ferrite hardening response in low alloy DP steels [23-24]. Therefore, the hardening behavior of ferrite microphase in ferrite-martensite DP steels has been one of the attractive research areas in physical metallurgy and has been addressed by several investigators [25-26]. Fereiduni et al.[27] have reported that a considerable variation in ferrite hardening response has also occurred within ferrite-martensite site DP microstructures containing various ferrite volume fractions. Kumar et al.[20] have reported that the mechanical behavior of low alloy ferrite-martensite DP steels is related to the size of ferrite grains and concluded that the density of dislocation had been significantly decreased from the ferrite-martensite interfaces to the central region of ferrite grains. Therefore, the hardening response of ferrite in ferrite–martensite DP steels has been reported to be affected with those parameters influencing the formation of geometrically necessary dislocations generated within ferrite during martensitic phase transformation, and so the role of some other variable parameters such as ferrite morphology, ferrite volume fraction and ferrite carbon concentration on the hardening response of ferrite in DP steels have not been followed considerably[27-30].

Ferrite and martensite microphases are associated with different levels of carbon and another alloying element partitioning during austenite to ferrite phase transformation, thus having different effects on the microstructural features and so mechanical properties of heat-treated DP steels [31-33]. Although, the carbon partitioning between ferrite and prior austenite during step-quench heat treatment can have severe effects on the austenite to ferrite phase transformations, the step-quench temperature and time, the steel chemical composition, and the partitioning of substitutional allowing elements are other questionable parameters in the field of ferrite and martensite hardening mechanisms and consequently the microstructural and mechanical properties of DP steels[21,29,31]. These arguments are still under war, and there is not a good agreement in this field of research work[21,34-36]. Accordingly, in the present study, it has been tried to find out the ferrite hardening variation in relation to ferrite carbon and silicon partitioning in the ferrite-martensite DP microstructures using a commercial grade of low alloy medium silicon 35CHGSA steel under step-quenching heat treatment conditions.

2. Materials and experimental procedures

2.1. Steel Composition and Heat Treatment

The steel used in this investigation was a commercial grade of hot-rolled 35 CHGSA low-alloy, medium-silicon strap sample with 5mm thickness, and the chemical composition is shown in Table 1. The heat treatment schedules were designed to achieve various microstructures involving different volume fractions of ferrite, pearlite, and martensite microconstituents. At first, the samples were austenitized at 900°C for 15 min and then air-cooled (normalized) to room temperature to develop more starting homogeneous microstructural features in the proposed heat-treated samples. Then, after reaustenitizing at 900°C for 15 min, the samples were immediately step-quenched in a molten salt bath ($1NaNO_3$ and $1KNO_3$) at 750, 720, 700, and 680°C and soaked isothermally for holding time of 5 min in order to develop the partial decomposition of prior austenite to various volume fractions of ferrite and pearlite microconstituents before water quenching. Finally, the samples were quenched in water to achieve various volume fraction of martensite from the remaining prior metastable austenite regions, as schematically shown in Fig. 1.

2.2. Microstructural investigations

The metallography of heat-treated samples was

carried out on the transverse section relative to the rolling direction of as-received strap samples according to the ASTM E 3 standard. Polished samples were etched with a 2% Nital solution[37] to reveal the various microstructural features. The volume fractions of ferrite, pearlite, and martensite microphases were measured using the point count method according to the ASTM: E562 standard condition[20]. The microstructures were characterized using an Olympus-PMG3 optical microscope followed with a TESCAN-MIRA 3-XMU field-emission scanning electron microscope (FE-SEM) operating at an accelerated voltage of 15 kV. To qualitatively compare the level of carbon and silicon partitioning between ferrite and prior austenite area during austenite to ferrite phase transformation, the line scanning for carbon and silicon chemical analyses were carried out at various locations of ferrite and martensite microconstituents using the EDS technique. The Rockwell macrohardness measurements with a load of 150 kg were conducted on the heat-treated samples. Microhardness tests were also carried out at various locations within ferrite grains, with a load of 1g being applied for 20 s duration loading time using a Future Tech microhardness tester machine model FM700.

Table 1. The chemical composition of investigated low alloy medium silicon commercial grade of 35CHGSA steel (in wt%).

	C	Si	Mn	S	P	Cr	Mo	Ni	Fe
	0.35	1.25	0.89	0.01	0.01	1.18	0.01	0.04	96.2

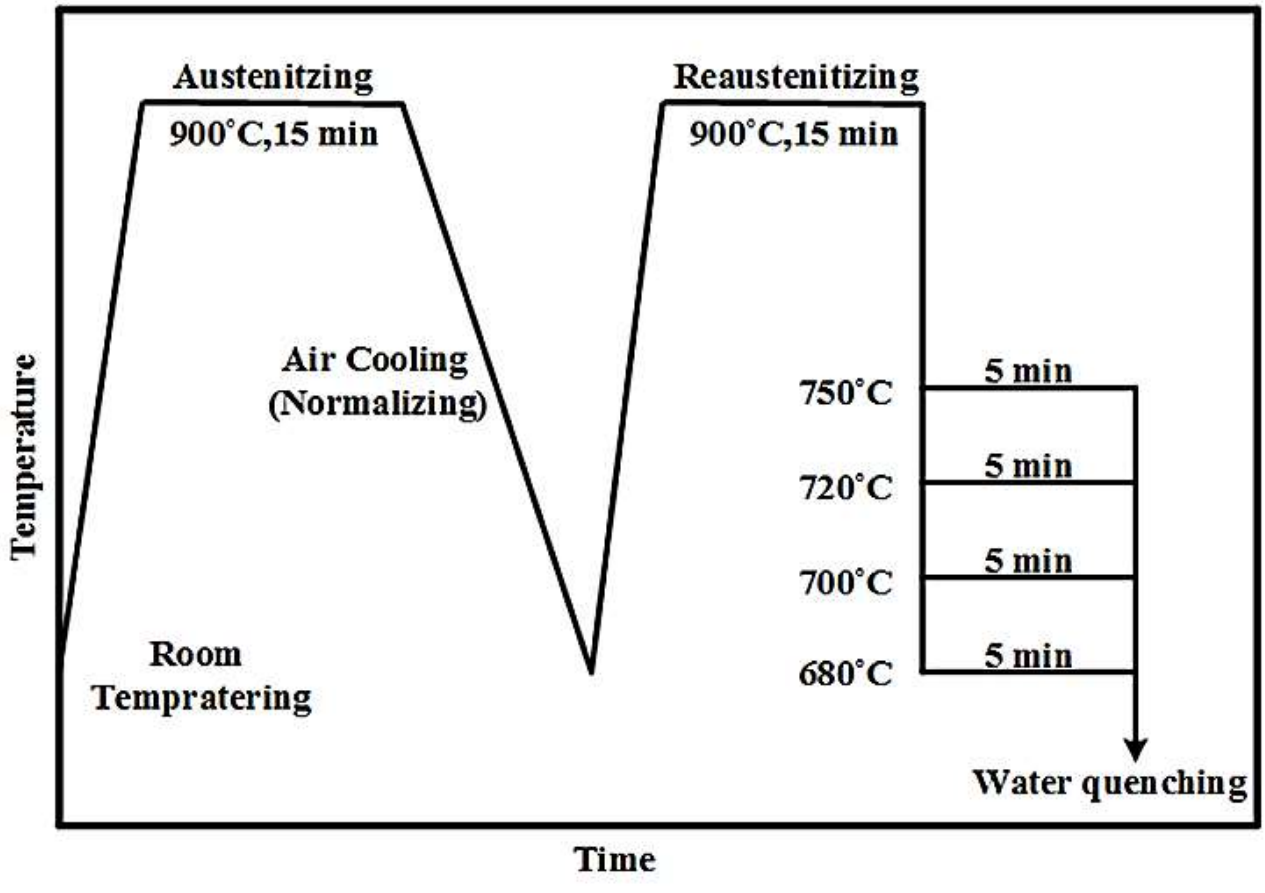

Fig. 1. Schematic diagrams of the heat treatment cycles.

3. Results and Discussion

3.1. Optical micrographs and hardness measurements

Figure 2 shows typical light micrographs in association with macrohardness taken from the heat-treated samples subjected to the application of step-quenching phase transformation of prior austenite over a wide range of isothermal temperatures for a constant duration of 5 min holding time. As it is obvious, these microstructures have composed a mixture of three completely different colored areas involving, white, gray, and contrasted brown ones which ones which corresponding to the microphages of ferrite, perlite, and martensite, respectively. The processes of ferrite, perlite, and martensite formation are as following: at first, after austenitizing the samples at 900°C for 15 min, the microstructure is completely austenite and then during step-quenching in the molten salt bath at isothermal temperatures of 750, 720, 700 and 680°C, depending on the temperature and holding time, ferrite nucleates and grows from the prior austenite grain boundaries.

The nucleation and growth of ferrite can be associated to the significant level of carbon partitioning between the ferrite and adjacent prior austenite areas, resulting in carbon-enriched austenite phase in which the nucleation and growth of pearlite can be occurred within these areas during prolong isothermal holding time. Finally, by cooling the samples in water, all of the remaining prior austenite areas are transformed into the martensite, and therefore, the triple-phase microstructures containing ferrite, perlite, and martensite microphases are formed. Depending on the isothermal holding time and temperature, if there is not enough holding time for carbon partitioning and perlite formation during the step-quenching condition, the perlite formation is not occurred, and eventually, the ferrite and martensite microphases are developed in the DP microstructures on the subsequent water quenching. In this way, Figure 2 shows typical representative light micrographs of various step-quench heat-treated samples, with the associated macrohardness data illustrating microstructural evolutions taking place during isothermal holding for 5 min at: 750; 720; 700; and 680°C followed by water quenching.

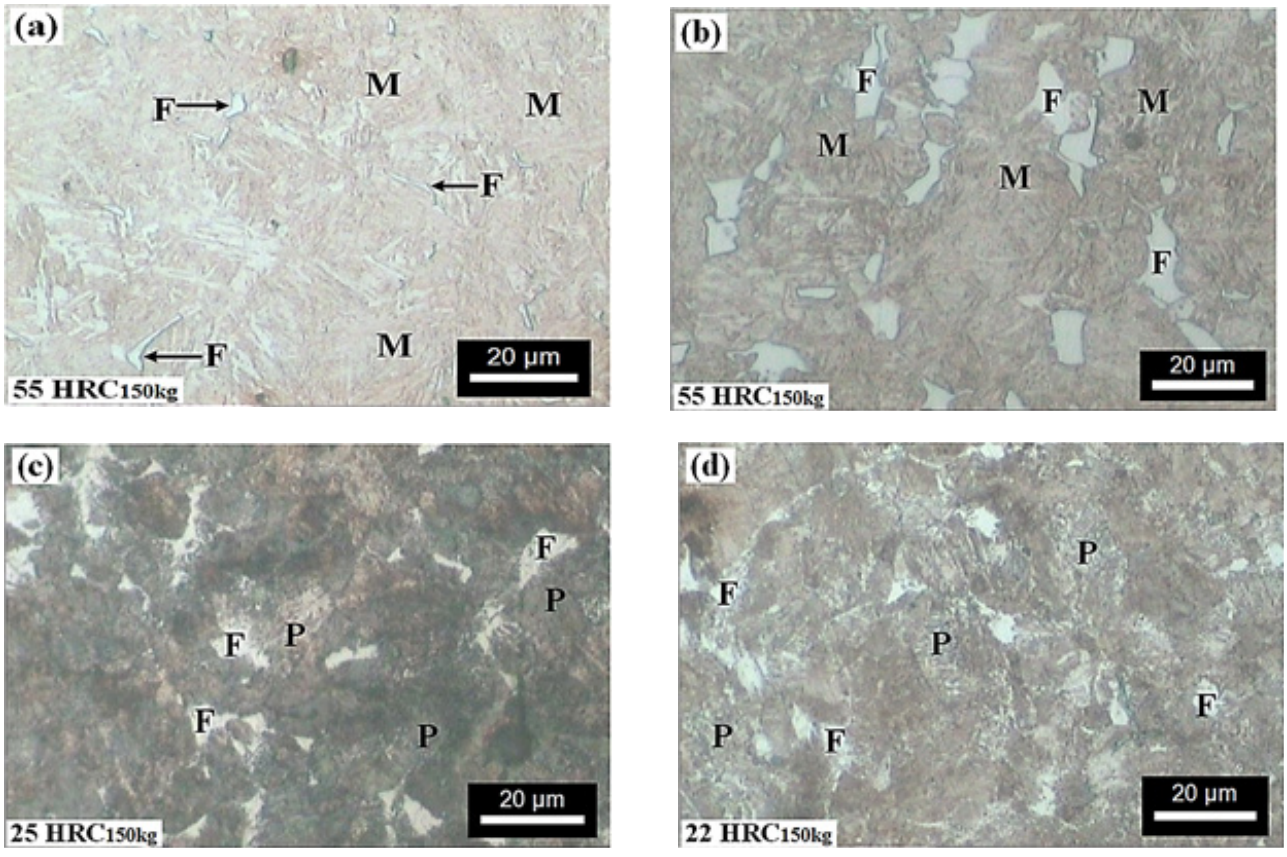

Fig. 2. Typical optical micrographs of various step-quench heat-treated samples, with the associated macrohardness data illustrating microstructural evolutions taking place during isothermal holding for 5 min at: 750; 720; 700; and 680°C followed by water quenching. Ferrite, pearlite, and martensite microconstituents are marked with F, P, and M symbols, respectively.

Figures 3(a) and (b) show the changes in hardness and volume fraction of ferrite as a function of isothermal step-quenching temperature of molten salt bath for the samples kept at a constant duration of 5 min holding time, respectively. As the step-quenching temperature of molten salt bath increases from 680 to 700°C, the hardness of heat-treated samples moderately increases from 22 to 25HRC and then sharply increases to the maximum value of 55HRC, which is related to the ferrite martensite DP samples involving 6% ferrite. With a further increasing in isothermal temperature from 720 to 750°C, the hardness has been abnormally remained unchanged around 55 HRC while the ferrite volume fraction decreases from 6 to 1%.

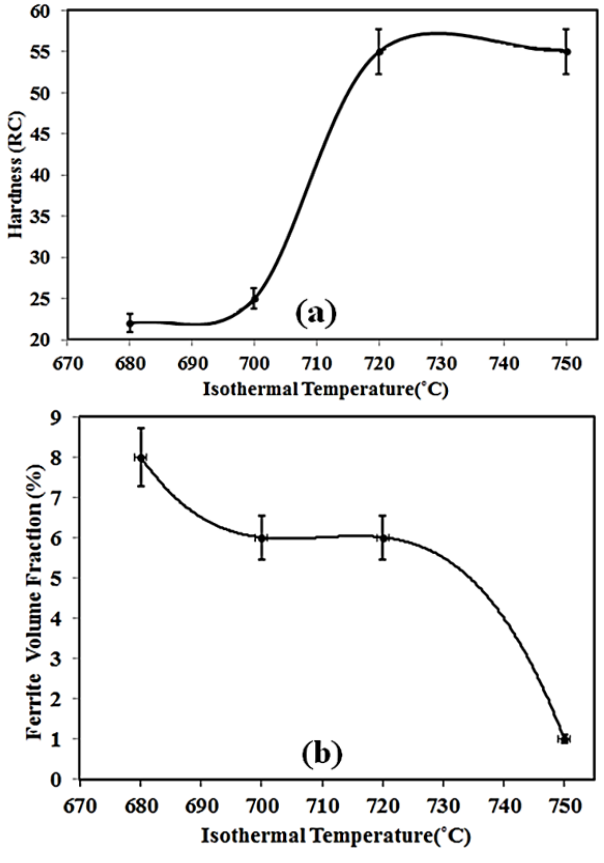

Fig 3. Changes in: (a) hardness and (b) volume fraction of ferrite, as a function of isothermal step-quenching temperature for the heat-treated samples kept in the molten salt bath for 5 min. The maximum hardness is abnormally developed in the ferrite-martensite DP samples with 6% ferrite corresponding to 720°C heat-treated condition.

3.2. Electron microscopy and carbon partitioning

Since the phase transformation of austenite to ferrite is a type of solid to solid diffusional phase transformation and can be associated with the partitioning of carbon and alloying elements between ferrite and adjacent prior austenite areas, the change in concentrations of carbon and silicon atoms was detected within the ferrite and martensite microphases formed in the DP microstructures. For this purpose, the EDS linear analyses of carbon and silicon were extensively performed at various locations within the ferrite grains in conjunction with the adjacent martensite areas, which corresponding to the carbon and silicon partitioning occurred during prior austenite to ferrite phase transformation. For this purpose, Fig 4 shows a typical scanning electron microscopy image with the superimposed locations at which the EDS line analysis was carried out within ferrite grain and the adjacent martensite areas in the step-quenching heat treatment samples at 720°C for 5 min. Figure 4a shows the DP microstructure consisting of ferrite grain (F) and martensite (M) areas along with the locations at which the EDS analysis was carried out for taken from carbon and silicon atoms. In this way, Figs 4b and c show the elemental analyses of carbon and silicon atoms, respectively. These results are reported as carbon and silicon concentration gradient graphs along the test line, which indicates the changes in carbon and silicon concentrations within the α grain, the α/γ interfaces, and the martensitic regions adjacent to the ferrite grain. Although, the measurement of carbon concentration by EDS analysis technique has been accompanied with some more overestimation, but this technique can be used as a comparative study in order to investigate the variation of carbon partitioning within ferrite and prior austenite areas[4,5,21,38]. As can be seen in Fig 4b, the carbon concentration within the central region of ferrite grain is maximum and decreases significantly to its minimum value as the spot location approaches the ferrite regions close to the α/γ interfaces. These results indicate that in comparison with the relatively homogeneous distribution of carbon atoms within the central regions of ferrite grain, a significant concentration gradient for carbon has been developed in the ferrite and martensite areas adjacent to the α/γ interfaces.

Figure 4c also shows the change in silicon concentration from the central martensite regions toward the α/γ interfaces and then to the ferrite grain. As can be observed during austenite to ferrite phase transformation, the concentration of silicon from the central region of ferrite grain to the α/γ interfaces was significantly decreased from 0.88 to 0.45 EDSNs. These results indicate that during the austenite to ferrite phase transformation process, the silicon partitioning was occurred from the central region of ferrite grain toward the α/γ interfaces in the same fashion as to the carbon partitioning (Fig. 4). The same trend in carbon and silicon partitioning, which is in good agreement with the researcher's view of how austenite to ferrite and austenite to perlite phase transformations take place[39].

Can be rationalized to the fact that the Si atom is a strong ferrite stabilizer element which is more distributed within α during the transformation of γ to α. Since the difference in size of Si and Fe atoms is such large that the high concentration of Si in α causes severe distortion within the lattice crystal of ferrite atoms so that the carbon atoms can be easily accommodated within the higher vacancy space developed between the ferrite atoms. Thus, during the γ to α phase transformation, the carbon atoms are more partitioned on the side of the austenite area adjacent to the α/γ interfaces. On the other hand, the carbon-poor ferrite area can be developed within the silicon poor ferrite area adjacent to the α/γ interfaces. The gradient of carbon concentration in the ferrite and martensite areas adjacent to the α/γ interfaces are significantly decreased from 6.10 to 2 EDSNs and 12 to 2 EDSNs, recpectively.

It is interesting to point out that the higher solubility of carbon atoms within the central ferrite areas can be associated to the higher distortion generated within ferrite crystal by higher silicon atoms. The lattice parameters of silicon and iron atoms are 0.543[33] and 0.287 nm[34] respectively, which shows that the crystalline lattice parameter of silicon is more than 65% larger than that the iron lattice parameter. With higher solubility of silicon in the α phase, a large level of irregularity is created in the iron crystal which increases the crystalline defects. Since the carbon atom is distributed as an interstitial atom in the crystalline defects of ferrite iron crystal, the crystalline defects increase as the Si concentration increases in the α phase causing higher carbon concentration within the higher Si ferrite areas.

3.3. Ferrite hardening variation

To examine the ferrite hardening variation, the microhardness test has been conducted at several locations within a particular ferrite grain in a particular step-quenching samples. A typical light micrograph shown in Fig. 5 is an example of followed microhardness procedure, representing hardness impressions taken from both locations (the central ferrite grains and the ferrite areas close to the prior α/γ interfaces) within several ferrite grains in the step-quench samples at 720°C for 5 min. It can be clearly seen that the minimum microhardness test values are related to the central position of ferrite grains, and it is increased with microhardness position close to the prior α/γ interfaces, indicating that the deformation resistance of ferrite grain is quite variable depending on the location of microhardness test. In this way, as

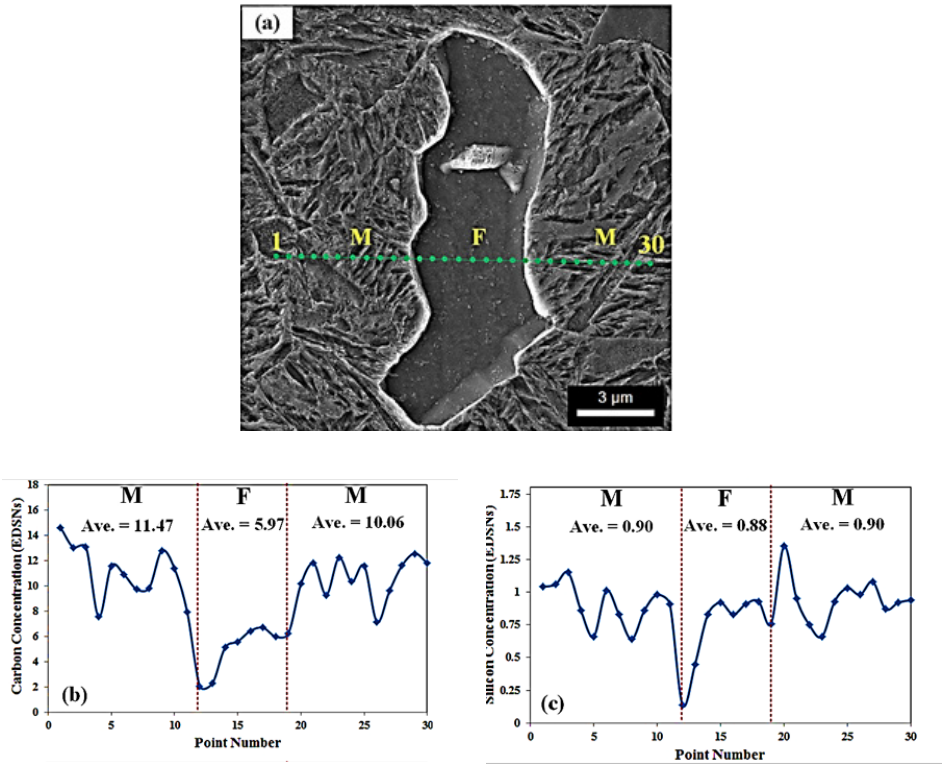

Fig. 4. (a) Typical electron micrograph with superimposed EDS spot-line scanning for: (b) carbon; and (c) silicon chemical analyses showing the variation of carbon and silicon concentrations in terms of EDS numbers (EDSNs) within the ferrite grain, and the adjacent martensite regions in the ferrite-martensite step-quench heat-treated samples at 720°C for 5 min. The carbon and silicon concentrations of the central ferrite region were quite variable in accordance with the carbon and silicon concentration of ferrite areas adjacent to the α/γ interfaces. F: Ferrite; M: Martensite.

microhardness location test has been changed from the central ferrite grains toward the ferrite areas close to the prior α/γ interfaces (Fig. 5), the ferrite hardening response has been significantly increased from 122 to 145HV_{1g} for the samples step-quenched at 720°C for isothermal holding time of 5 min. For more information concerning the ferrite hardening variation, the EDS line scan analyses were carried out at different locations within the ferrite grains and adjacent martensite areas, as illustrated in Fig. 4 for the samples heat-treated at 720°C for holding time of 5 min. The average carbon and silicon concentrations from the central location of ferrite grains toward the ferrite areas close to the prior α/γ interfaces have been decreased from 5.97 to 4.11 EDSNs and 0.88 to 0.45 EDSNs, respectively (Fig. 4a, Fig. 4b).

The experimental results indicate that the ferrite hardness has been significantly increased from the central location of a particular ferrite grain toward the ferrite areas close to the prior α/γ interfaces, while the carbon and silicon concentrations are adversely decreased from the central ferrite areas toward the ferrite regions adjacent to the α/γ interfaces (Figs. 4, 5). The nearer ferrite location is to the prior α/γ interfaces, the more is ferrite hardening response, while the lowers are carbon and silicon concentrations. This abnormal ferrite hardening response can be moderately affected by the partitioning of carbon and silicon atoms between ferrite and prior austenite areas indicating that another ferrite hardening mechanism rather than carbon and silicon solid solution hardening should be operated in the ferrite grains developed in the ferrite-martensite DP microstructures. On the other hand, the carbon and silicon concentrations within a specific ferrite grain have been decreased from the central position of ferrite grain toward the prior α/γ interfaces (Fig. 5 and 4). This indicates that a significant contribution to the higher ferrite hardening developed within the ferrite areas close to the prior α/γ interfaces cannot be considered for carbon and silicon partitioning, occurred between ferrite and prior austenite during diffusional phase transformation of austenite to ferrite. This variation in ferrite hardness can be attributed to the other ferrite hardening mechanisms such as ferrite/martensite interaction involved in the martensitic phase transformation adjacent to the ferrite areas.

It is a well-known fact that a significant level of volume expansion can be occurred during martensitic phase transformation in the prior austenite areas adjacent to ferrite grains. The martensitic phase transformation can induce a significant level of plastic deformation and unpinned geometrically necessary dislocations within the ferrite areas for maintaining lattice continuity[40-41]. These heterogeneously distributed dislocations are partly mobile and contribute in part to the higher ferrite hardening response developed in the ferrite-martensite DP microstructures[42]. With increasing plastic deformation, the dislocation density build-up and the accumulated dislocation zones are established resulting a dislocation cell network through all of the ferrite grains. Therefore, at least some of the adjacent ferrite areas have to be deformed plastically owing to volume expansion during austenite to martensitic phase transformation. After such phase transformation-induced deformation, residual stresses are remained in the ferrite areas due to the inhomogeneity of plastic deformation throughout the ferrite grains, resulting the geometrically necessary dislocations cause local hardening in ferrite areas[25].

In summary, the experimental results presented in this study show that by reducing the volume fraction of soft ferrite phase from 6 to 1%, the hardness of ferrite-martensite DP samples is constant. This abnormal hardening phenomenon can be rationalized to the mutual effect of carbon partitioning on ferrite and martensite hardening variation developed during isothermal holding in the step-quenching molten salt bath. On the one hand, by increasing the volume fraction of soft ferrite phase in the ferrite-martensite DP microstructures, the hardness decrease in the samples because of higher ferrite formation, but on the other hand, by increasing the volume fraction of ferrite, more carbon partitioning can be developed between ferrite and the adjacent prior austenite areas causing much harder martensite formation on the subsequent water quenching. Therefore, the overall hardening effect of higher carbon martensite formation is greater than the softening effects of ferrite.

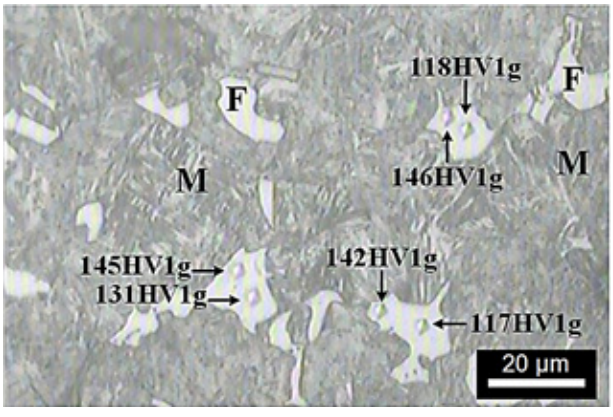

Fig. 5. Typical light micrograph with superimposed locations of microhardness tests in association with ferrite microhardness data showing the variation in ferrite hardness within the particular ferrite grains taken from the particular ferrite-martensite DP samples obtained at 720°C for isothermal holding time of 5 min. A higher ferrite hardening response occurred within the ferrite regions close to the α/γ interfaces in comparison to the central regions of ferrite grains. The ferrite microhardness data are measured with a constant loading force of 1 g. F: Ferrite; M: Martensite.

4. Conclusions

In the present work, the phase transformation of austenite to ferrite and so the partitioning of carbon and silicon atoms between ferrite and prior austenite were investigated in a commercial grade of medium silicon low alloy ferrite-martensite DP steel particularly focusing on the ferrite hardening variation. The conclusions are as followings:

- Performing step-quench heat treatment cycles for constant period of 5 min holding time at isothermal temperatures of 750 and 720°C leads to the formation of ferrite-martensite DP microstructures involving 1 and 6%Vol fraction, while at lower isothermal step-quench temperatures of 700 and 680°C, the formation of ferrite-perlite microstructures with volume percentages of 6 and 8% ferrite are developed in the microstructures, respectively.
- With increasing isothermal temperature of step-quench heat treatment cycles from 680 to 750°C for constant duration of 5 min, the hardness DP samples have been increased from 22 to 55 HRC. The maximum value of hardness is related to the ferrite-martensite DP samples involving 6% of soft ferrite phase. With increasing isothermal temperature behind that of 750°C, the hardness is surprisingly remained unchanged at 55 HRC in the samples involving full martensite microstructures.
- The ferrite hardening response is quite variable within a particular ferrite grain in a particular ferrite-martensite DP sample. The average ferrite microhardness from the central location of ferrite grains toward the ferrite area near the prior α/γ interfaces has been increased from 122 to 145HV_{1g} for DP samples treated at 720°C for 5 min holding time.
- During phase transformation of prior austenite to ferrite, a significant level of carbon and silicon partitioning has been developed between ferrite and prior austenite areas. The carbon and silicon concentrations from central regions of ferrite grains toward the α/γ interface are decreased from 5.97 to 4.14 EDSNs and 0.89 to 0.45 EDSNs, respectively.
- The gradient of carbon concentration in the ferrite and martensite areas adjacent to the α/γ interfaces are significantly changed from 6.10 to 2 EDSNs and 12 to 2 EDSNs, recpectively.

Reference

[1] T. Baudin, C. Quesne, J. Jura, and R. Penelle: Mater. Charact., 47(2001), 365.

[2] E. Ahmad, T. Manzoor, K. L. Ali, and J. Akhter: J. Mater. Eng. Perform., 9(2000), 310.

[3] E. Ahmad and R. Priestner: J. Mater. Eng. Perform., 7(1998), 776.

[4] A. S. Ghorabaei and S. G. Banadkouki: Mater. Sci. Eng. A., 700(2017), 562.

[5] E. Fereiduni and S. G. Banadkouki: Mater. Design., 56(2014), 232.

[6] O. Abedini, M. Behroozi, P. Marashi, E. Ranjbarnodeh, and M. Pouranvari: Mater. Res., 22(2019).

[7]M. Alipour, M. A. Torabi, M. Sareban, H. Lashini, E. Sadeghi, A. Fazaeli: Mech. Based. Des. Struc., (2019), 1.

[8] S. Sakai, S. Morito, T. Ohba, H. Yoshida, and S. Takagi: J. Alloy. Compd., 577(2013), S597.

[9] J.-Y. Kang, S.-J. Park, D.-W. Suh, and H. N. Han: Mater. Charact., 84(2013), 205.

[10] O. Majidi, F. Barlat, Y. P. Korkolis, J. Fu, and M.-G. Lee: Met. Mater. Int., 22 (2016), 968.

[11] F. Fernandes, D. Oliveira, and A. Pereira: Procedia. Manufacturing.,13(2017), 219.

[12] C. Lesch, N. Kwiaton, and F. B. Klose: steel. res. int., 88(2017), 1700210.

[13] C. C. Tasan, M. Diehl, D. Yan, M. Bechtold, F. Roters, L. Schemmann: Mater. Res., 45(2015), 391.

[14] F. Maresca, V. Kouznetsova, and M. Geers: J. Mech. Phys. Solids., 73(2014), 69.

[15] X. Li, L. Shi, Y. Liu, K. Gan, and C. Liu: Mater. Sci. Eng. A., (2019), 138683.

[16] M. Balbi, I. Alvarez-Armas, and A. Armas: Mater. Sci. Eng. A., 733(2018), 1.

[17] C. Trevisiol, A. Jourani, and S. Bouvier: Metallography, Microstructure, and Analysis., 8(2019), 123.

[18] C. A. Salvador, E. S. Lopes, J. Bettini, and R. Caram: Mater. Lett.,189(2017), 201.

[19] B. Bramfitt and P. Mangonon: Dallas, Tex, 15-16 Feb., (1982), 1982.

[20] E 562-02, Annual Book of ASTM Standards, 03.01(1993).

[21] A. Ebrahimian and S. G. Banadkouki: Mater. Sci. Eng. A., 677(2016), 281.

[22] S. Monia, A. Varshney, S. Sangal, S. Kundu, S. Samanta, and K. Mondal: J. Mater. Eng. Perform., 24(2015), 4542.

[23] Z. Jiang, Z. Guan, and J. Lian: J. mater. sci., 28(1993), 1814.

[24] A. Bag, K. Ray, and E. Dwarakadasa: Metall. Mater. Trans. A., 30(1999), 1193.

[25] J. Kadkhodapour, S. Schmauder, D. Raabe, S. Ziaei-Rad, U. Weber, and M. Calcagnotto: Acta. Mater., 59(2011), 4387.

[26] Y. S. Byun, I. S. KIM, and S. J. KIM: T. Iron. Steel. I. Jpn., 24(1984), 372.

[27] E. Fereiduni and S. G. Banadkouki: J. Alloy. Compd., 589(2014), 288.

[28] D. Ji, M. Zhang, D. Zhu, S. Luo, and L. Li: Mater. Sci. Eng. A., 708(2017), 129.

[29] A. Ebrahimian and S. G. Banadkouki: J. Alloy. Compd., 708(2017), 43.

[30]S. Kumar, A. Kumar, R. Madhusudhan, R. Sah, and S. Manjini: J. Mater. Eng. Per., 28(2019), 3600.

[31]D. Barbier, L. Germain, A. Hazotte, M. Gouné, and A. Chbihi: J. mater. sci., 50(2015), 374.

[32]J. Kang, Y. Ososkov, J. D. Embury, and D. S. Wilkinson: Scripta. Mater., 56(2007), 999.
[33]A. Nouri, H. Saghafian, and S. Kheirandish: J. Iron. Steel. Res. Int., 17(2010), 44.
[34]X.-L. Cai, A. Garratt-Reed, and W. Owen: Metall. Trans. A., 16(195), 543.
[35]J. Speer, E. De Moor, and A. Clarke: Mater. Sci. Tech., 31(2015), 3.
[36]A. Ghaheri, A. Shafyei, and M. Honarmand: Mater. Design., 62(2014), 305.
[37]G. F. Vander Voort: Metallography. microstructures., 9(2004).
[38]M. Ferrante and R. Doherty: Acta. Metall., 27(1979), 1603.
[39]V. Vaks, A. Y. Stroev, V. Urtsev, and A. Shmakov: J. Exp. Theo. Phys., 112(2011), 961.
[40]M. Calcagnotto, D. Ponge, E. Demir, and D. Raabe: Mater. Sci. Eng. A., 527(2010), 2738.
[41]A. Sarosiek and W. Owen: Mater. Sci. Eng. A., 66(1984), 13.
[42]H. Bhadeshia: Acta. metall., 29(1981), 1117.